International Journal of Industrial Electronics and Control.
ISSN 0974-2220 Volume 3, Number 2 (2011), pp. 135-150

http://www.irphouse.com

Performance of Induction Motor Field-Weakening Operation Using the Q-axis Current Added Flux Reference Technique

Feri Yusivar and Shinji Wakao

Universitas Indonesia , Waseda University, Japan
**Corresponding Author: Electrical Engineering Department,*
Universitas Indonesia, Kampus UI Depok, Indonesia 16424
E-mail: yusivar@ee.ui.ac.id, yusivar@yahoo.com

Abstract

The high-speed operation of the field oriented induction motor control requires a flux decreasing to counteract the back electromotor force (EMF) increasing that will approach the available inverter voltage. Decreasing the flux causes the available torque is reduced. However, the available torque is still can be improved by implementing the voltage saturation strategy to maximize the dc-bus voltage utilization. The field weakening can be performed automatically using a voltage controller without utilizing any motor parameter. Unfortunately, in this field weakening scheme the saturation strategy is not easy to be implemented.

In this paper, a novel field-weakening scheme based on saturated voltage control strategy is proposed and its performance comparison with the one based on voltage control strategy (without implementing the saturation strategy; later we call it as the previous scheme to distinguish it with the proposed scheme) is presented. The applied object of both schemes in this paper is a sinusoidal pulse width modulated (SPWM) voltage source inverter (VSI)-fed induction motor drive. Though the proposed scheme is quite simple, it is effective to provide a higher torque capability then the previous scheme does. The maximum torque is produced by increasing the flux-producing current as much as possible while the stator voltage reference is saturated. The voltage saturation condition is stimulated by adding the torque-producing current into the flux-producing current reference. Experiments were carried out to verify the proposed scheme. The experimental results of the previous scheme were also presented for comparison purposes.

Keywords: Saturated voltage, Maximum torque, Flux weakening, Induction motor, Drive system.

Introduction

In a torque-controlled induction motor drive, the maximum output torque and output power besides depend on the motor power rating, also depend on the inverter current rating and the maximum voltage that the inverter can supply to the machine. When the inverter power capability is higher than the machine power, it should be limited to keep operating the machine safely. To operate the machine at very high speed as required in many applications, such as the traction and spindle drives, field-weakening scheme should be adopted, but available torque is reduced. A control strategy, which considers current and voltage limitations, should be implemented so that a maximum torque can be obtained in the whole speed range.

Many papers have proposed new control strategies to provide a maximum torque capability in the field weakening area with taking into account the current and voltage limits[1]~[4]. The approaches have superior torque capability compare to the conventional $1/\omega_r$ method. To achieve a maximum torque, the flux reference is calculated by examining the relation of the output torque capability with the leakage inductance of the machine[1]. A different approach in determining the flux reference is using a voltage controller[2],[3]. Then, a voltage-margin controller is developed that rejects dc-link and load disturbances[4]. However, all field-weakening schemes[1]~[4] are applied only in the linear region of the PWM inverter.

Since the space vector pulse width modulation (SVPWM) becomes popular used in motor drive system, the study of the SPWM capability, especially for the field-weakening application, is left behind. Although many papers have been dealt with the maximizing voltage utility of PWM inverter through an overmodulation operation[5]~[12], their implementation with the field-weakening scheme in the induction motor drive has been not studied intensively. Only few studies on it were found[13],[14]. An over modulation strategy by tracking the voltage vector along hexagon sides of SVPWM was incorporated with the field-weakening scheme to give a better voltage utilization[13]. However, here the field-weakening scheme that was adopted[1] still uses motor parameters to set the flux reference. It was not mentioned a possibility the use of the voltage control strategy as the authors proposed[3]. In another reference, a voltage saturation technique was used for maximizing dc-bus utilization in current regulator[14]. Here, a form of field weakening is provided intrinsically by using a complex vector synchronous frame PI current regulator. Unfortunately, the current limitation is not considered in this technique. And also a scheme for determining the flux reference is still required.

This paper proposes a different approach of field-weakening control for providing a maximum torque capability considering voltage saturation and current limitation. The voltage saturation performs a voltage limitation with maximum dc-bus utilization. In present time, the proposed scheme is implemented to the rotor-flux oriented control of a SPWM VSI-fed induction motor. The first part of the paper describes the currents control with decoupling system. Then followed by describing the voltage saturation strategy and the field-weakening scheme in detil. The final part of the paper presents the experimental results of the proposed scheme including comparisons with the previous scheme.

Currents control with decoupling system

The dynamics of an induction motor in the synchronous frame are given by

$$\dot{x} = Ax + Bu \tag{1}$$

where

$$x = [i_{ds}^e \quad i_{qs}^e \quad \phi_{dr}^e \quad \phi_{qr}^e]^T \ , \ u = [v_{ds}^e \quad v_{qs}^e]^T$$

$$A = \begin{bmatrix} a_{11} & a_{12} & a_{13} & a_{14} \\ -a_{12} & a_{11} & -a_{14} & a_{13} \\ a_{31} & 0 & a_{33} & a_{34} \\ 0 & a_{31} & -a_{34} & a_{33} \end{bmatrix}, \ B = \begin{bmatrix} b_1 & 0 \\ 0 & b_1 \\ 0 & 0 \\ 0 & 0 \end{bmatrix}$$

$$a_{11} = -R_s/(\sigma L_s) - L_m^2/(\sigma L_s L_r T_r) \ , \ a_{12} = \omega_e$$

$$a_{13} = L_m/(\sigma L_s L_r T_r) \ , \ a_{14} = \omega_r L_m/(\sigma L_s L_r)$$

$$a_{31} = L_m/T_r \ , \ a_{33} = -1/T_r \ , \ a_{34} = \omega_{sl}$$

$$b_1 = 1/(\sigma L_s) \ , \ \sigma = 1 - L_m^2/(L_s L_r)$$

i_{ds}^e , i_{qs}^e d-q axes stator currents in the synchronous frame;

ϕ_{dr}^e , ϕ_{qr}^e d-q axes rotor fluxes in the synchronous frame;

v_{ds}^e , v_{qs}^e d-q axes stator voltage in the synchronous frame;

L_s , L_r , L_m stator, rotor, and mutual inductances;

R_s , R_r stator and rotor resistances;

ω_e , ω_r electrical and rotor angular frequency;

ω_{sl} slip frequency $(\omega_e - \omega_r)$;

T_r rotor time constant (L_r/R_r) .

The rotor-flux-oriented control is achieved by letting $\phi_{qr}^e = 0$ and $\phi_{dr}^e = \phi_r^e =$ constant. Then, the current dynamic equations (1)

yield:

$$\sigma L_s (di_{ds}^e/dt) = -R_s i_{ds}^e + \omega_e \sigma L_s i_{qs}^e + v_{ds}^e \tag{2}$$

$$\sigma L_s (di_{qs}^e/dt) = -R_s i_{qs}^e - \omega_e \sigma L_s i_{ds}^e - \omega_e L_m \phi_{dr}^e / L_r + v_{qs}^e \tag{3}$$

The feed forward decoupling control method is to choose inverter output voltages such that

$$v_{ds}^{e*} = (K_p + K_i/s)(i_{ds}^{e*} - i_{ds}^e) - \sigma L_s \omega_e i_{qs}^e \tag{4}$$

$$v_{qs}^{e*} = (K_p + K_i/s)(i_{qs}^{e*} - i_{qs}^e) + \sigma L_s \omega_e i_{ds}^e + (1-\sigma) L_s \omega_e \phi_{dr}^e / L_m \tag{5}$$

where the proportional and integral gains are set to $K_p = \sigma L_s / T_d$ and $K_i = R_s / T_d$, as for the stator currents to have a first order delay response of their references with time constant of T_d.

Then, to minimize loop feedback systems, the currents feedback used for decoupling system including the back EMF compensation can be estimated using

$$i_{ds1}^{e*} = i_{ds}^{e*} /(1+T_d s) \tag{6}$$

$$i_{qs1}^{e*} = i_{qs}^{e*} /(1+T_d s) \tag{7}$$

$$i_{ds2}^{e*} = i_{ds1}^{e*} /(1+T_r s) \tag{8}$$

and then

$$\omega_e = \omega_r + R_r i_{qs1}^{e*} /(L_r i_{ds2}^{e*}) \tag{9}$$

$$\phi_{dr}^{e} = L_m i_{ds2}^{e*} \tag{10}$$

The block diagram of the currents control with decoupling system is shown in Fig. 1. This configuration will be used in this paper as a standard currents control system, so that only the field-weakening scheme of the proposed strategy will be different compared with one of the previous strategy.

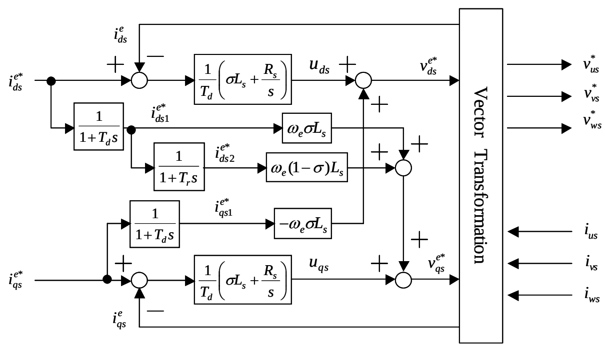

Fig. 1 Currents control with decoupling system.

Voltage saturation technique

The SPWM signal is constructed by comparing a high-frequency triangular carrier with three reference signals. It can be easily implemented as an analog or a digital solution; hence it makes high flexibility in practical use.

With index modulation m = 1, SPWM provides voltage utility about 78% of the value that would be reached by square-wave (six step) operation. The dc-bus utilization can be increased through the use of zero-sequence harmonics addition[7], square wave addition[9], or reshaping the modulation command[11]. However, it is preferred to use the saturation technique instead, due to its simplicity, especially when it implemented with the field-weakening scheme. The saturation technique can be realized quite simple by limiting the phase voltage reference to the value of $v_{dc}/2$ as shown in Fig. 2. In this way, the need to overmodulate in the pulse-dropping region is eliminated. Fig. 2 shows the half period SPWM construction of the saturated and unsaturated voltage reference. For the saturated voltage reference case, the amplitude is enlarged and then is limited to not exceed the triangle carrier amplitude. As a result the effective output voltage is boosted.

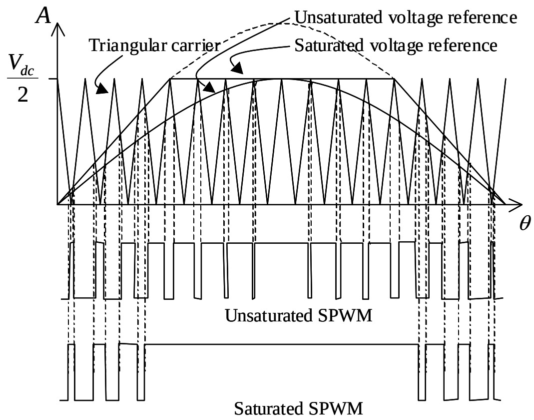

Fig. 2 Sinusoidal pulse width modulation.

As the current control system described in previous section, the saturation technique illustrated in Fig. 2 will be used in this paper as a standard of voltage limiter. In the previous field-weakening scheme that will be described later, the voltage limiter is still necessary to anticipate an overshoot phenomenon of the voltage controller in transient.

Field-weakening scheme

Constraints in Operating Conditions Induction motor can operate in one of three operating modes: torque constant mode, power constant mode, and voltage constant mode. Below the rated speed (torque constant mode) the motor operation is current-limited. In power constant mode the motor operation is both current-limited and voltage-limited as the back-EMF approaches the maximum inverter voltage while the current is still limited. In voltage constant mode the speed becomes so high that the current cannot exceed the maximum inverter current anymore.

Current and voltage limitations are available in inverter by means of overcurrent and overvoltage protections. However, we still have to limit the motor operation below those over current and over voltage values. Otherwise the protection system will shut down the inverter. Thus it is useful to limit the motor operation in the controller system.

The machine current operation is limited to a maximum stator current $i_{s\max}$ that is the minimum of inverter maximum current and motor maximum current. This current limitation is provided by limiting q-axis current reference i_{qs}^{e*}, which the priority is given to d-axis current reference i_{ds}^{e*}, and follows the equation expressed in (11). The field weakening technique determines the d-axis current reference i_{ds}^{e*} which is limited to its rated value.

$$i_{ds}^{e*2} + i_{qs}^{e*2} \le i_{s\max}{}^2 \tag{11}$$

The voltage applied to the motor is limited to v_{smax} that depends on the available dc-bus voltage v_{dc} and pulse-width modulation (PWM) strategy. The motor voltage input follows the following equation.

$$v_{ds}^{e*2} + v_{qs}^{e*2} \le v_{s\max}{}^2 \tag{12}$$

The steady-state voltage equations of the induction motor in the synchronously rotating reference frame are given by

$$v_{ds}^{e*} = R_s i_{ds}^{e*} - \omega_e \sigma L_s i_{qs}^{e*} \tag{13}$$

$$v_{qs}^{e*} = R_s i_{qs}^{e*} + \omega_e L_s i_{ds}^{e*} \tag{14}$$

In high-speed operation, the stator resistance effect is negligible in (13) and (14). Then the current-limit constraint of (11) and the voltage-limit constraint of (12) can be rewritten as the following equations.

$$(i_{ds}^{e*}\omega_e L_s)^2 + (i_{qs}^{e*}\omega_e \sigma L_s)^2 \le v_{s\max}{}^2 \tag{15}$$

$$\left(\frac{v_{ds}^{e*}}{\omega_e \sigma L_s}\right)^2 + \left(\frac{v_{qs}^{e*}}{\omega_e L_s}\right)^2 \le i_{s\max}{}^2 \tag{16}$$

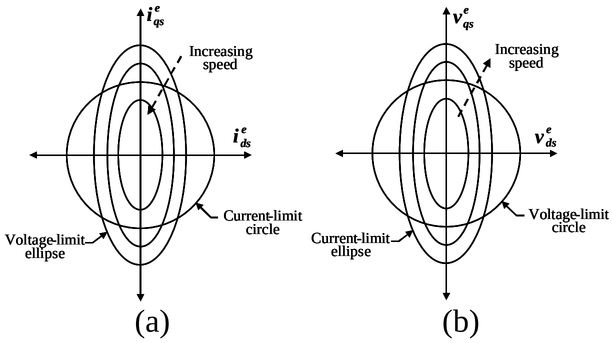

Fig. 3. (a) Current boundary (b) Voltage boundary.

Eq. (11) and (12) mean the circle equations, while Eq. (15) and (16) mean the ellipse equations. Fig. 3 shows the current-limit and voltage-limit boundaries in the q^e-d^e current and voltage planes.

Maximum torque capability The maximum torque provided by the field-weakening scheme based on voltage control strategy, which considering the current limit and voltage limit, was described clearly by Kim and Sul[3]. The whole field-weakening region can be divided into two sub regions: region I ($\omega_{base}<\omega_e\le\omega_1$) and region II ($\omega_e>\omega_1$). In the field-weakening region I, the maximum output torque is obtained by the locus of the optimal voltage vector which moves rightward along the boundary of the voltage-limit circle as the operating frequency increases (from point A to point B as shown in Fig. 4). In the field-weakening region II, the maximum output torque is obtained only by the voltage-limit constraint as regardless of the operating frequency (at point B; not point C as shown in Fig. 4).

$$v_{qs}^{e*} = |v_{ds}^{e*}| = V_{s\max}/\sqrt{2} \tag{17}$$

Now, if the voltage saturation strategy can be implemented with the field-weakening scheme, the voltage-limit boundary is enlarged as shown in Fig. 4. As the results, the base frequency ω_e becomes higher and the field-weakening area is widened. Without voltage saturation, the field-weakening operation starts at point A. Since the voltage limit v_{smax} become larger when the saturation strategy is used, the field-weakening operation starts at point A1 with higher v_{ds}^{e*} and v_{qs}^{e*} compared the ones at point A. The higher voltage references the higher base frequency, according to Eq. (13) and (14). Then, more voltage available more power will available. Hence, for the same required torque the higher maximum frequency can be reached, since the mechanical power is

$$P_{mech} = T_e \omega_r \tag{18}$$

It means the field-weakening area is widened. In general, the torque capability is improved by maximizing the dc-bus voltage utilization. For instance, as shown in Fig. 4, a higher torque can be achieved at point B1 with implementing the saturation strategy rather than at point B without implementing the saturation strategy.

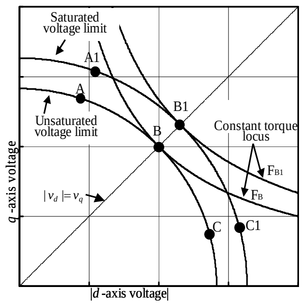

Fig. 4. Voltage vector for producing maximum torque.

The previous field-weakening scheme The voltage control strategy for providing maximum torque in the field weakening operation is implemented using two Proportional-Integral (PI) controllers[3] as shown in Fig. 5. One (PI_1) controls the field-component current i_{ds}^{e*} to adjust the machine input voltage not exceeding the maximum voltage V_{smax} and following Eq. (12). Since the SPWM is used, V_{smax} is $\sqrt{3/2}(mV_{dc}/2)$ or v_c^* is set to $\sqrt{3/2}(mV_{dc}/2)$, where m is index modulation and $\sqrt{3/2}$ is the vector transformation factor. PI_1 controller input is $V_{s\max}^2 - (v_{ds}^{e**2} + v_{qs}^{e**2})$ to avoid the square-root computation. The other (PI_2) controls the maximum value $I_{q\max}$ of the torque-component current i_{qs}^{e*} to adjust v_{ds}^{e*}, so that follows the current limit of Eq. (17), when the field-weakening region II is entered. PI_2 controller input is $0.5V_{s\max}^2 - v_{ds}^{e**2}$ to avoid the square-root computation as in PI_1 controller. Besides i_{ds}^{e*} is fed to the d-axis current controller, it is also used to perform the current limiter as in Eq. (1). Then the limit value of Limiter2 is the minimum of $\sqrt{I_{s\max}^2 - i_{ds}^{e*2}}$ and the PI_2 output.

Before the three-phase voltage references are fed to the SPWM inverter, each phase voltage reference is limited to $V_{dc}/2$ to guarantee the voltage reference amplitude doesn't exceed the triangle carrier amplitude. Although the voltage has been limited by PI_1, the voltage limiter (Limiter3) is still necessary to anticipate an overshoot phenomenon of the voltage controller in transient. The limited voltage references are then transformed to the synchronous frame again and become the voltages feedback for the voltage controllers (PI_1 and PI_2).

Voltage limitation will deteriorate the currents control performance since it causes an integrator windup phenomenon. To prevent integrator windup the "realizable references"[14] or "back-calculation"[15] method can be used. However, it is not needed in our proposed voltage limitation, since: first, the feedback voltages used by the field-weakening scheme (voltage controller) are the saturated voltage references and second, the phase voltage references are guaranteed not to exceed the triangle carrier amplitude. Therefore, the PWM outputs always linear with the input of the saturated voltage references.

The anti-windup strategy is applied in PI_1 since i_{ds}^{e*} is limited to its rated value by Limiter1 (torque constant mode operation). However, a simpler way to prevent integrator windup can also be used instead. Here, when the control output reaches its limitation value, the integrator initial values of the controller for next iteration are reset to the initial values from previous iteration. This anti-windup strategy should also be applied in the speed controller if the torque reference T_e^* is provided by a speed controller, since the torque reference is limited by Limiter2.

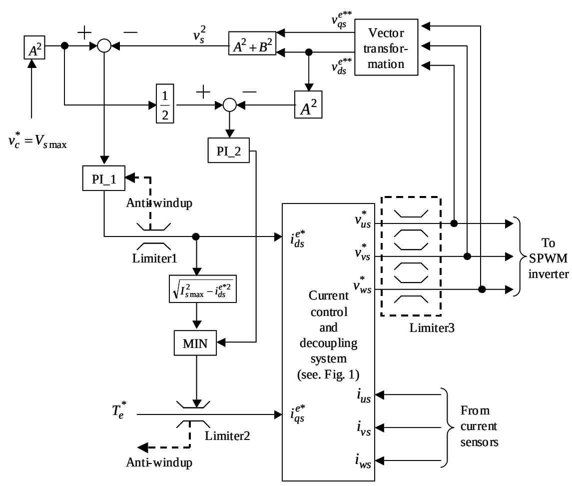

Fig. 5. Field-weakening scheme based on voltage control strategy (previous scheme).

The proposed field-weakening scheme The problem that we are faced now, is how to combine the voltage control strategy[3] with the voltage saturation strategy as simple as possible. In the previous field-weakening scheme, the voltage saturation condition is difficult to be performed, since PI_1 controls the voltage to follow the voltage reference ($V_c^*=V_{s\max}$). The saturation condition occurs only when the voltage overshoot occurs. Although it is possible to enlarge the voltage reference ($V_c^*>V_{s\max}$), it is better if the voltage is only enlarged when a higher or maximum torque is required, not permanently. In another word, the available voltage should be varied proportional with the required torque. As an advantage, the voltage saturation condition only occurs when a high or maximum torque is required.

Field weakening control reduces the *d*-axis current reference in order to keep the voltage not exceed its maximum value. If it is seen in the opposite direction, the voltage will increase when the flux reference increase. Now if we assume a positive disturbance is added to the flux-producing current reference, the voltage controller (PI_1 in Fig. 5) will compensate it so that the voltage will be still kept constant and a saturated condition will be not achieved. In this case the flux will not increase and neither the torque. Then to achieve a saturated condition, a perfect controller like a PI controller should not be used. For this purpose a P (proportional) controller is used for the voltage controller instead of PI controller. As a result, a small steady state voltage error will occur and if a positive disturbance is added to the flux reference the voltage will be slightly increase proportional to the disturbance. If the voltage level greater than the limiter voltage, it will be saturated. Thus the effective voltage as seen by the motor is boosted.

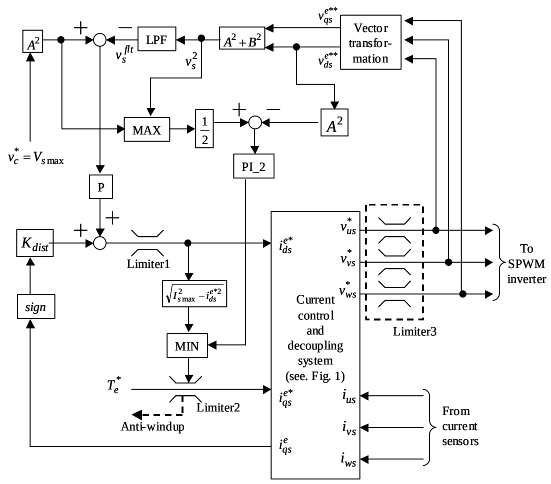

Fig. 6. Field-weakening scheme based on saturated voltage control strategy (proposed scheme).

In the steady state of field weakening area, the torque equation for the power-invariant form can be expressed as

$$T_e = N_p \frac{L_m^2}{L_r} i_{ds}^{e*} . i_{qs}^{e*} = k . v_{ds}^{e*} . v_{qs}^{e*} \tag{19}$$

where $k = -N_p L_m^2 / (\sigma L_s^2 L_r \omega_e^2)$ and N_p is pole pairs number. As seen in Eq. (19) the torque is proportional to the product of $i_{ds}^{e}*$ and $i_{qs}^{e}*$. It means the torque also depends on the flux. The higher flux is produced the higher torque is produced. Since $i_{qs}^{e}*$ is the torque producing current reference, the *q*-axis current i_{qs}^{e} will corresponds with the produced torque. Then if the i_{qs}^{e} is added to $i_{ds}^{e}*$ as disturbance, it will affect the flux, and then it will also affect the torque as a positive feedback signal. Since in the rotor flux oriented control the *d*-axis current i_{ds}^{e} is always positive value, the disturbance should be always positive value. It means the magnitude of *q*-axis current i_{qs}^{e} only should be used as a disturbance. Fig. 6 shows block diagram of the proposed field-weakening scheme based on saturated voltage control strategy.

As seen in Fig. 6, a first order low-pass filter (LPF) with a cut-off frequency of 100 Hz filters the stator voltages firstly to improve the voltage control performance, since a P controller is used. The flux reference of the proposed strategy is expressed as

$$i_{ds}^{e*} = K_{vp}(v_c^{*2} - v_s^{flt}) + signK_{dist}i_{qs}^{e} \tag{19}$$

where: *sign* = 1 if $i_{qs}^{e} \geq 0$ and *sign* = -1 if $i_{qs}^{e} < 0$. K_{vp} represents the proportional gain, v_s^{flt} is the filtered signal of the sum of squared *d*-axis and *q*-axis voltages, v_c^{*} is set to V_{smax}, and K_{dist} is the disturbance gain.

Since the available voltage of the proposed field-weakening scheme is varied, the reference value for PI_2 should be modified as shown in Fig. 6. Here, the maximum of V_{smax} and

$\sqrt{v_{ds}^{e**2} + v_{qs}^{e**2}}$ is chosen.

Experimental results

Experimental setup To validate the proposed scheme, experiments were carried out. And to verify it has an improved torque capability over the previous scheme, the comparison experimental results are also presented. The test motor is a three-phase, four-poles, 750 W, 1410 rpm IM with the specifications listed in Table 1. All algorithms are implemented by the embedded 'C' code in a floating point DSP (Texas Instruments TMS320C32, operating speed 50MHz). An incremental encoder with 4096 ppr is mounted on the shaft for detecting the rotor position. The circle time (full control time) of whole experimental system is 0.1 milliseconds (sampling period is 0.1 milliseconds). The rotor speed and the speed control are sampled every 1 millisecond using an interrupt method.

Table 1. Induction motor parameters.

750W, 200V, 4poles, 50Hz, 1410 rpm		
R_s 2.76 Ω	R_r 2.9 Ω	Total inertia 0.0586 kg.m^2
L_s 234.9 mH	L_r 234.9 mH	L_m 227.9 mH

Maximum torque test The block diagram of experimental system is shown in Fig. 7. The motor is run from a standstill condition with the torque reference is set to its maximum (rated torque) for 15 seconds and then set to zero torque (see Fig. 8.). This will forces the field-weakening scheme to provide a maximum torque in the whole motor operation.

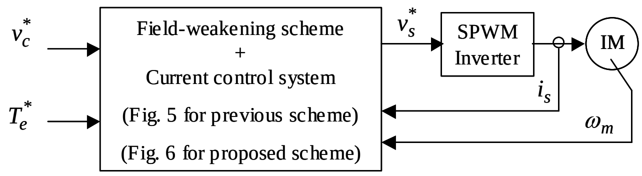

Fig. 7. Block diagram of the experimental system.

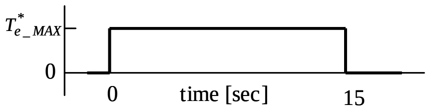

Fig. 8. Torque reference for maximum torque test.

Fig. 9 and 10 show the experimental results of the maximum torque test operation of induction motor using the previous and proposed field-weakening scheme respectively. The base frequencies achieved by the previous and the proposed schemes are 1274.4 rpm and 1420.9 rpm, respectively. The maximum frequencies achieved by the previous and the proposed schemes are 6679.7 rpm and 7133.8 rpm. These results confirm that a higher base frequency and a widened field-weakening area are produced by the proposed scheme. This can be explained by comparing Fig. 9(d) with Fig. 10(d). The output voltages produced by the proposed scheme are larger than by the previous scheme. Fig. 9(e) and 10(e) show that the voltage locus of maximum torque moves along the voltage limit circle in region I and kept at the point of v_q=|v_d| when the region II is entered.

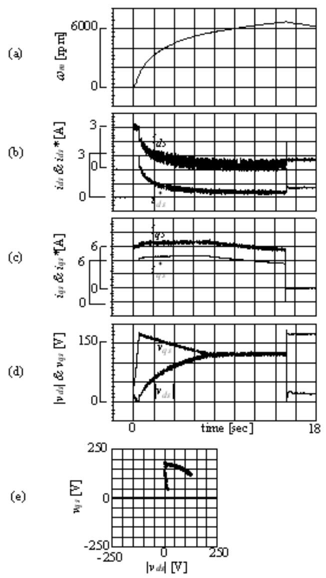

Fig. 9. Experimental results of field-weakening operation based on unsaturated voltage control (previous scheme).

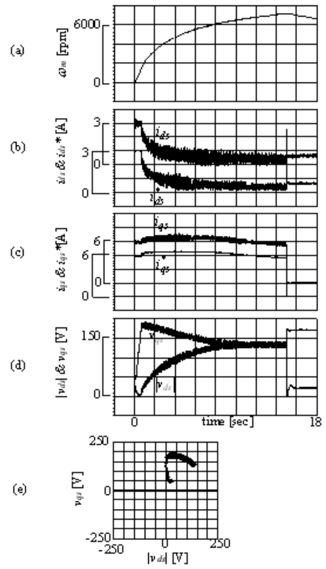

Fig. 10. Experimental results of field-weakening operation based on saturated voltage control (proposed scheme).

Noise effect In the proposed field-weakening scheme, the saturation condition is stimulated by disturbing the flux current reference with the q-axis current i_q. The performance of the flux current will be deteriorated by the current noise in i_q. The noise effect in the field-weakening operation using the proposed scheme can be seen in Fig. 10(b) compared to Fig. 9(b). The ripple of i_{ds}* by the proposed scheme was large. Although it did not really affect the d-axis current response (ripple of i_{ds} by proposed scheme was relatively same with one of i_{ds} by previous scheme), the same condition will be very difficult to be achieved if the motor power is large. Large motors have large leakage factor and currents. This situation affects noise conditions of the motor caused by the structure of the motor or by the electromagnetic interference (EMI). Large noise will cause the high performance of field-weakening operation very difficult to be achieved.

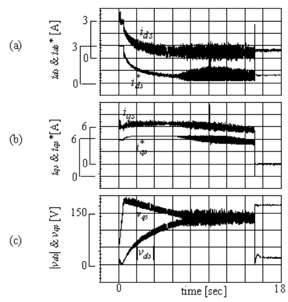

Fig. 11. Noise effect investigating results when the voltage saturation condition is stimulated by i_{qs}*.

To overcome the noise effect, the torque-producing current reference i_{qs}* can be used to replace i_{qs} as disturbance in stimulating a voltage saturation condition. Fig. 11 shows the investigation results of the noise effect when the voltage saturation condition is stimulated by i_{qs}*. As it is supposed, the ripple of i_{ds}* can be eliminated in field-weakening region I, comparing i_{ds}* of Fig. 11(a) with of Fig. 10(b). It is also less than the ripple of i_{ds}* by previous scheme in Fig. 9(b). However, when region II is entered the ripple of i_{ds}* in Fig. 11(a) becomes worse. This is because of the instability of the PI_2 controller. The control gains were not suitable anymore. It was found that the PI_2 control gain selection is critical, not only for the proposed scheme, but for the previous scheme too. For that reason we propose a new control strategy for the operation in region II.

Fig. 12 shows the block diagram of the new control strategy for field-weakening operation in region II. The controller only uses an integrator with conditions. The input of integrator is $|v_{qs}*|$-$|v_{ds}*|$ and the output is used to adjust the maximum current, so that the voltages are kept to be $|v_{qs}*|=|v_{ds}*|$ when the field-weakening operation enters to region II. The integrator gain of 0.5 is selected. The selection of integrator gain is not critical. It can be used as it in all configurations in this paper, including the configuration with the i_{qs} disturbance for stimulating the voltage saturation condition. The factor of 0.8 in the conditions of integrator is to provide a hysteresis band.

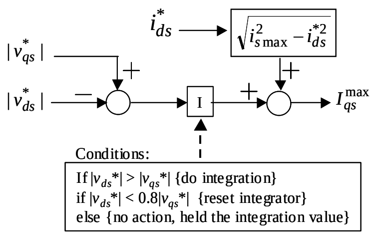

Fig. 12. New control strategy for region II.

Fig. 13 shows the implementation results of the new control strategy for the field-weakening operation in region II. It is seen that the ripple of i_{ds}* and i_{qs}* occur when the region II is entered are eliminated by using the new control (comparing Fig. 13 with Fig. 11). These results are very important according to the application of the proposed field-weakening scheme with a large power motor.

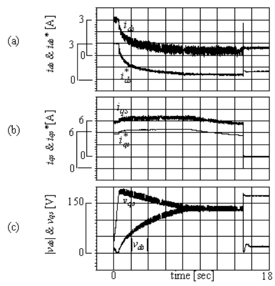

Fig. 13. Experimental results of the new control strategy application for region II.

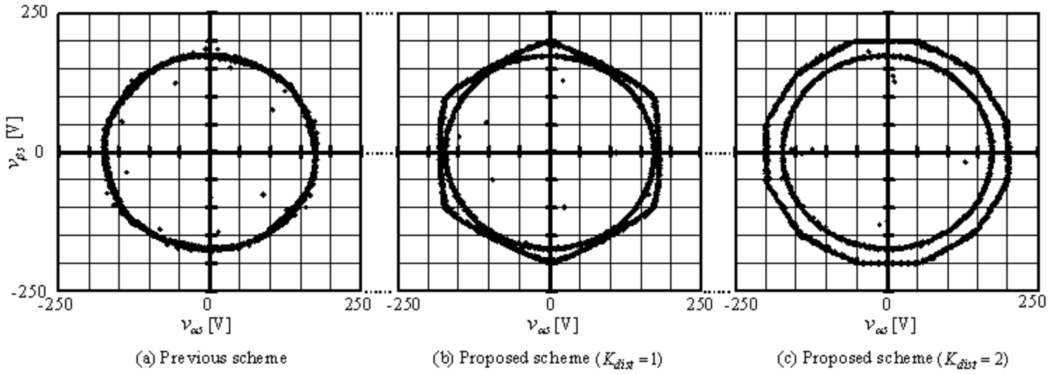

Fig. 14. Locus of stationary voltages $v_{\alpha s}$ versus $v_{\beta s}$ when T_e changed from maximum torque to zero torque (Time: 13 Sec ~ 16 Sec)

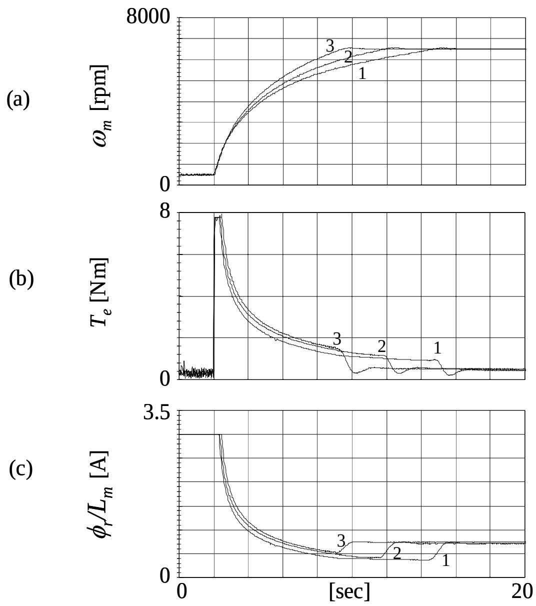

Fig. 15. Speed, torque, and flux comparisons:

1. Conventional scheme
2. Proposed scheme (K_{dist}=1)
3. Proposed scheme (K_{dist}=2)

Behavior in torque requirement As mentioned before, in the proposed field-weakening scheme, the voltage saturation condition only occurs when a higher or maximum torque is required. This statement is proven by looking to the locus of stationary voltages when the torque changed from maximum to zero torque condition as shown in Fig. 14.

In the conventional scheme, the voltage saturation condition is not achieved. Therefore, the voltage locus always tracks the circle of voltage limit as shown in Fig. 14(a). When the proposed scheme is applied, in the maximum torque condition the voltage limit boundary becomes a hexagon (in case the disturbance gain K_{dist}=1) and automatically returns to a circle when the maximum torque is not required anymore as shown in Fig. 14(b). The advantage of this situation, besides the torque capability is improved; the harmonic losses can be reduced in the high-speed operation when the maximum torque is not required (see the small ripple of experimental results in period time of 15~18 seconds of Fig. 13). Fig. 14(c) shows the voltage locus in case the disturbance gain K_{dist}=2. The voltage limit boundary becomes a 12-gon when the maximum torque is required and returns to a circle when the maximum torque is not required.

Speed control operation Finally, the proposed scheme is tested with the speed control implementation. Fig. 15 shows the speed, torque, and flux comparisons of the speed control operation. The speed reference is changed from 500 rpm to 6500 rpm. It is proven that the proposed scheme provides a higher torque and flux. As a result, a higher speed response is achieved as shown in Fig. 15(a).

Conclusion

Disturbing the flux-producing current reference with the torque-producing current reference while the stator voltage is limited or saturated, higher voltage availability can be provided, since the dc-bus voltage utilization is maximized. As a result, a higher torque is provided and the flux-weakening region is widened. Experimental results confirm the validity of the field-weakening scheme based on saturated voltage strategy. The voltage saturation condition only occurs when a higher or maximum torque is required. The maximum torque is produced by increasing the flux-producing current as much as possible. As the conclusion, the proposed scheme is verified to provide an improved torque capability over the previous field-weakening scheme using a voltage control strategy.

The stability analysis and control design of the field- weakening scheme proposed in this paper are the challenges for our future works. The implementation of another method in maximizing the dc-bus utility for improving the torque capability in the field-weakening operation is still interesting to be investigated. Furthermore, its implementation with the speed sensorless system is still open to be studied.

Reference

[1] S.-H. Kim, S. K. Sul, and M. H. Park: “Maximum torque control of an induction machine in the field weakening region,” *IEEE Trans. Ind. Appl.*, vol. 31, no. 4, pp. 787-794, (1995)

[2] H. Grotstollen and J. Wiesing: "Torque capability and control of a saturated induction motor over a wide range of flux weakening," *IEEE Trans. Ind. Electron.*, vol. 42, no. 4, pp. 374-381, (1995)
[3] S-H. Kim and S-K Sul: "Voltage Control Strategy for Maximum Torque Operation of an Induction Machine in the Field-Weakening Region," *IEEE Trans. Ind. Electron.*, vol. 44, no. 4, pp. 512-518, (1997)
[4] B.J. Seibel, T.M. Rowan, and R.J. Kerkman: "Field-Oriented Control of an Induction Machine in the Field-Weakening Region with DC-Link an Load Disturbance Rejection," *IEEE Trans. Ind. Appicat.*, vol. 33, no. 6, pp. 1578-1584, (1997)
[5] R.J. Kerkman, D. Leggate, B.J. Seibel, and T.M. Rowan: "An Overmodulation Strategy for PWM Voltage Inverters," in *IECON'93, 19th Int. Conf. Ind. Electron., Contr. Instrumentation*, Maui, Hawaii, Nov. 15-19, pp. 1215-1221, (1993)
[6] J. Holtz, W. Lotzkat, and A.M. Khambdkone: "On Continuous Control of PWM Inverters in the Overmodulation Range Including the Six-Step Mode," *IEEE Trans. On Power Elec.*, vol. 8, no. 4, pp. 546-553. (1993)
[7] S. Halasz, G. Csonka, A.A.M. Hassan: "Sinusoidal PWM Techniques With Additional Zero-Sequence Harmonics," in *IECON'94, 20th Int. Conf. Ind. Electron., Contr. Instrumentation*, pp. 85-90. (1994)
[8] R.J. Kerkman, T.M. Rowan, D. Leggate, and B.J. Seibel: "Control of PWM Voltage Inverters in the Pulse Dropping Region," *IEEE Trans. on Power Elec.*, vol. 10, no. 5, pp. 559-565. (1995)
[9] V. Kaura and V. Blasko: "A New Method to Extend Linearity of a Sinusoidal PWM in the Overmodulation Region," *IEEE Trans. on Ind. Applicat.*, vol. 32, no. 5, pp. 1115-1121. (1996)
[10] S. Bolognani and M. Zigliotto: "Novel Digital Continuous Control of SVM Inverters in the Overmodulation Range," *IEEE Trans. on Ind. Applicat.*, vol. 33, no. 2, pp. 525-530. (1997)
[11] V. Kaura: "A New Method to Linearize Any Triangle-Comparison-Based PWM by Reshaping the Modulation Command," *IEEE Trans. on Ind. Applicat.*, vol. 33, no. 5, pp. 1254-1259. (1997)
[12] D.C. Lee and G.M. Lee: "A Novel Overmodulation Technique for Space-Vector PWM Inverter," *IEEE Trans. on Power Elec.*, vol. 13, no. 6, pp. 1144-1151. (1998)
[13] B.H. Bae, S.H. Kim, and S.K. Sul: "A New Overmodulation Strategy for Traction Drive," in IECON'99, *25th Int. Conf. Ind. Electron., Contr. Instrumentation*, pp. 437-442. (1999)
[14] F. Briz, A. Diez, M.W. Degner, and R.D. Lorenz: "Current and Flux Regulation in Field-Weakening Operation," *IEEE Trans. on Ind. Applicat.*, vol. 37, no. 1, pp. 42-50. (2001)
[15] L. Harnefors, and H.P. Nee, "Model-based current control of ac machines using the internal model control method," IEEE Trans. on Ind. Applicat., vol. 34, no. 1, pp. 133-141. (1998)